

---

# Chapter 2

## Materials and Methods

### Part I Functional Magnetic Resonance Imaging

---

<b>2.1 Non-invasive neuroimaging techniques.....</b>	<b>62</b>
<b>2.2 The physics of NMR and MRI.....</b>	<b>63</b>
2.21 Spin .....	63
2.22 Net magnetisation.....	65
2.23 Radiofrequency magnetic fields.....	65
2.24 Relaxation .....	67
2.25 Image formation: frequency and phase encoding .....	70
2.26 Voxels .....	71
2.27 Image contrast .....	72
2.28 Ultrafast MRI sequences: Echo-Planar Imaging.....	72
<b>2.3 fMRI and the magnetic properties of blood .....</b>	<b>74</b>
2.31 BOLD contrast in fMRI .....	74
2.32 Neurophysiology and BOLD .....	75

## 2.1 Non-invasive neuroimaging techniques

Recording the electrical activity of the human brain using scalp electrodes, a technique referred to as electroencephalography (EEG), is widely used in clinical practice and experimental neuroscience. This non-invasive technique is, however, limited by the inability to precisely localise the source of electrical activity. Magnetoencephalography (MEG), a non-invasive technique which records the minute fluctuations in magnetic fields produced by electrochemical activity in the brain, provides better spatial resolution than scalp-recorded EEG. However, at present the most widely used techniques for mapping functional neuroanatomy are those that employ a metabolic metric to indirectly measure neuronal activity. The two principal techniques are positron emission tomography (PET), and functional magnetic resonance imaging (fMRI). PET uses exogenous radiolabelled substances injected into the bloodstream to measure regional cerebral blood flow (rCBF) whereas fMRI relies on endogenous contrast mechanisms to produce a measure of local levels of blood oxygenation, the blood oxygenation level dependent (BOLD) signal. The temporal and spatial resolution of the BOLD signal are better than that afforded by PET measurements of rCBF. Given that the aim of this thesis was to investigate the hippocampal response to novelty, imaging time-dependent responses to novelty in this relatively small neuroanatomical structure required the best possible spatial and temporal resolution. Hence, all data in this thesis were acquired using fMRI.

## 2.2 The physics of NMR and MRI

fMRI is a special form of magnetic resonance imaging (MRI), used widely in clinical practice. Both fMRI and MRI rely on the principle of nuclear magnetic resonance (NMR), discovered independently by Bloch and Purcell in the 1940s (Purcell *et al.*, 1945; Bloch *et al.*, 1946). The first application of NMR as a topographic imaging technique was by Lauterbur (1973) who applied NMR of hydrogen atoms within histological specimens. This early study provided a basis for the use of MRI to image the structure of human tissue and, later, for the use of fMRI to measure brain activity. The basic physical principles underlying MRI and fMRI are very similar.

### 2.21 Spin

All nuclei possess the quantum quality spin. MRI techniques measure the effects of changing the spin of particular atomic nuclei, such as  $^1\text{H}$  and  $^{13}\text{C}$ , which have an odd number of protons. In living organisms, the most abundant source of protons is the hydrogen atom in the form of water. The hydrogen nucleus is positively charged and the spinning motion of this charge induces a local magnetic field. These hydrogen nuclei (or protons) therefore behave like small magnets, i.e. they have a magnetic moment. In the absence of a magnetic field, these individual spins are randomly orientated and the bulk material has no net magnetisation. However, in an externally applied magnetic field,  $B_0$ , the individual spins align with the external magnetic field. If the spin is not completely aligned with the direction of the magnetic field  $B_0$ , this causes the proton to revolve, or precess, around the field

direction (figure 2.1). The frequency with which the axis rotates around the field direction is called the resonance (or ‘Larmor’) frequency, and is directly proportional to the field strength  $B_0$ .

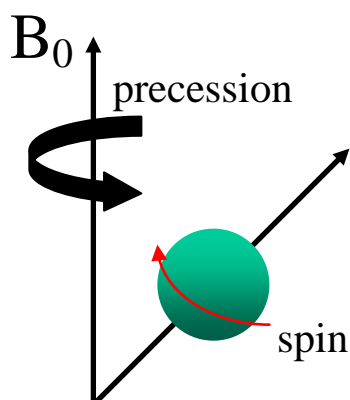


**Figure 2.1 Spin and precession of a single proton. The proton possesses the quantum quality spin (red arrow). In an external magnetic field, the proton precesses (black curved arrow) around the longitudinal magnetisation vector ( $B_0$ ).**

Quantum mechanics dictates that a spin can have different energies depending on the orientation of its magnetic moment with respect to the applied magnetic field: when the magnetic moment is aligned with the field, its energy will be lower than when it opposes the field. For the simple spin system of  $^1\text{H}$ , the magnetic moment can have two orientations with respect the magnetic field, either against it (high energy state) or along it (low, ground energy state). The amount of energy required to flip orientations is so small that the normal thermal energy available at room temperature is enough to flip spins. All of the signals generated in

MRI are, therefore, based on small differences between these energy states. The fact that the energy differences are small is one reason why MRI techniques tend to be safe but also why they are typically limited by signal strength.

### *2.22 Net magnetisation*

The sum over all the nuclei in an object volume gives the net magnetisation for the object. The description of the net magnetisation is based on a co-ordinate system, with the  $z$  axis being in the direction of the applied magnetic field. The resting net magnetisation is called the equilibrium magnetisation. In equilibrium, more spins are in the ground than in the high energy state. Summing the contributions of individual magnetic moments will, therefore, give a net magnetic moment along the direction of the applied magnetic field. Even though a small part of the rotating magnetisation of each nucleus has a component projecting into the  $xy$  plane, there is no equilibrium net 'transverse magnetisation' because the average magnetisation in this plane over all nuclei cancels to zero.

### *2.23 Radiofrequency magnetic fields*

Spins can be excited from the ground to the high energy state by applying an oscillating radiofrequency electromagnetic field ( $B_1$ ) perpendicular to the main magnetic field ( $B_0$ , applied in the  $z$  plane). To achieve the most efficient transfer of energy, the oscillation frequency of the  $B_1$  field should be the same as the spin resonance (Larmor) frequency (e.g. 63.9 MHz for a proton in a 1.5 Tesla field).

Modulating the proportion of spin energy states will change the direction of the net magnetisation vector. For rotation of the net magnetisation vector to occur,

two processes must take place simultaneously. First, protons are moved to the higher energy state until there are equal numbers of high and low energy spins. Second, the radiofrequency (RF) pulse rephases the protons so that they are brought into coherence (in phase). This has the effect of moving the net magnetisation vector into the transverse plane. The net magnetisation can now also be considered to rotate about this new applied radiofrequency magnetic field  $B_1$ , just as they did about the original, much larger field  $B_0$ . During this rotation, the angle from the original equilibrium direction along the  $z$  axis increases with time. By varying the amplitude and duration of the RF exposure, typically delivered in millisecond pulses, any desired angle can be produced. For example, if the  $B_1$  field is applied long enough to equilibrate the spin populations, the magnetisation vector will be zero and rotated into the  $xy$  plane. This is referred to as a  $90^\circ$  pulse, producing a  $90^\circ$  rotation of the net magnetisation – a  $90^\circ$  flip angle. For most angles from the equilibrium longitudinal magnetisation there will be a non-zero component of the magnetisation (the transverse magnetisation) in the  $xy$  plane. It is this transverse component that gives rise to a detectable NMR signal.

Following the above example, when the  $B_1$  field is turned off after this  $90^\circ$  pulse, the magnetisation vector will rotate about  $B_0$  in the  $xy$  plane with the spin resonance frequency. This is observable because the oscillating magnetic field induces a voltage in a coil positioned in the  $xy$  plane (Faraday's Law). MRI systems are designed to measure the transverse magnetisation, so the receiver coils, which may be the same as those used to apply the RF pulses, are sensitive only to the transverse component. The initial amplitude of the detected RF signal is proportional to the number of protons in the sample (the proton density). The greater the proton

density, the greater the magnetisation hence the greater the signal detected by the RF coils.

### 2.24 Relaxation

After excitation, the spin system will ultimately give off the absorbed energy and return to its equilibrium state with the magnetisation vector returning to its original position along the  $z$  axis. Hence, the strength of the signal detected by the RF coils, which is directly related to the amount of net transverse magnetisation, will gradually decay to zero. The molecular environment of the nuclei is reflected in the time variation of signal amplitude as the nuclei return to equilibrium. This release of energy happens gradually and occurs in two ways: (1) energy is given up to neighbouring *molecules* in the surrounding environment and is called spin-lattice relaxation, and (2) energy is given up to nearby *nuclei* and is called the spin-spin relaxation.

**T1 relaxation:** Spin-lattice or T1-relaxation describes the regrowth of the magnetisation vector along the  $z$  axis. This regrowth is an exponential process described by the T1 time constant. Protons that have been excited to the higher energy state dissipate this energy to molecules of the surrounding structure ('lattice') as heat. Protons returning to the lower energy state causes regrowth of the magnetisation vector along the  $z$  axis.

The exact composition of the environment will affect T1. For example, the protons in water have a longer T1 than those in fat because the carbon bonds in fat resonate near the Larmor frequency, which facilitates the transfer of energy to the

lattice. In the human brain, the different water content of grey and white matter (71% and 84%, respectively) means that T1 contrast can be used to provide contrast between these two tissues.

**T2 relaxation:** Spin-spin or T2-relaxation describes the disappearance of coherence of the magnetic moment in the  $xy$  plane (the transverse magnetisation,  $M_{xy}$ ), occurring at a different rate to the recovery of longitudinal magnetisation. The term spin-spin refers to the fact that interactions between protons determine the rate of T2 relaxation. No energy is actually lost; rather, energy is exchanged between protons, and there is a loss of “order” or entropy. As neighbouring spins pass energy from one to another, their rotations become desynchronised. Their slightly different rotation frequencies result in build-up of phase differences that gradually decrease  $M_{xy}$ . The loss of  $M_{xy}$  will always be faster than the longitudinal relaxation ( $T2 < T1$ ) because in addition to energy transfer to the lattice molecules, dephasing represents an extra mechanism of magnetisation cancellation.

**T2\* relaxation:** Dephasing will also occur if the applied magnetic field environment is non-uniform. In a non-uniform field, spins in different parts of the object will be rotating at different frequencies and quickly lose coherence (become dephased), possessing less net transverse magnetisation because of the resulting cancellation. This loss of transverse magnetisation due to inhomogeneous fields is often much shorter than the natural T2 signal decay and is characterised by another exponential time constant,  $T2'$ . The value of this time constant is determined by the technical implementation of the magnetic field and any field inhomogeneity caused by the



properties of the object itself.  $T2^*$  relaxation reflects the combination of  $T2$  and  $T2'$  signal decays. fMRI sequences usually measure  $T2^*$ .

The magnetic field contribution to the inhomogeneity giving rise to the  $T2'$  signal decay can be refocused with a spin echo, a  $180^\circ$  pulse along an axis in the  $xy$  plane at some time  $t$  after the initial  $90^\circ$  excitation pulse. Following this  $180^\circ$  'echo' pulse, the separate spin signals become more in phase and the signal becomes greater until time  $2t$  when all spins again have the same phase and the  $M_{xy}$  is temporarily again at a maximum. The time  $2t$  is called the echo time (TE). Echoes can be formed without  $180^\circ$  RF pulses by using magnetic field gradients to dephase and then rephase the spins. Adjusting the time of the dephase/rephase gradient balance allows the time of echo formation to be changed. This type of 'gradient echo' is often used in fast imaging sequences where it can produce faster echoes and use less RF power than spin echoes. All  $T2^*$  data presented in this thesis were acquired using this gradient-echo technique. In chapter 6 we see how varying the gradient echo time can increase the sensitivity of fMRI to anterior medial temporal lobe activity. Although the  $180^\circ$  pulses cancel out  $T2'$  effects due to magnetic field inhomogeneities, the recovered  $T2^*$  signal at the echo is still less than its original height as determined by the proton density. This is due to  $T2$ -relaxation, the second contribution to  $M_{xy}$  magnetisation dephasing, which cannot be refocused with a spin-echo because it results from spatial and temporal variations in the intrinsic magnetic environment of each spin.

### *2.25 Image formation: frequency and phase encoding*

Placing a sample within a homogenous  $B_0$  field will not produce tomographic MR images for the simple reason that all protons will experience (roughly) the same magnetic field and, hence, the frequencies of their emitted signal will all be identical. In MRI, a second magnetic field (called a gradient field) is applied so that protons within the sample will emit different frequency signals that are dependent on their spatial position. In other words, as the magnetic field varies across the object, the resonance frequencies of spins (their Larmor frequencies) also vary. The spins' resonance frequencies are, therefore, determined by their location along the gradient axis. The number of spins resonating at a particular frequency determines the amplitude of that frequency in the spectrum of observable resonance frequencies. For each frequency component of the measured signal, the known value of the applied gradient strength and direction can be used to calculate the position from which the signal came. Therefore, the spectrum of a sample placed in a magnetic field gradient will be a projection of the spin density along the gradient axis (Lauterbur, 1973). For clinical whole body imaging systems, the maximum linear field strength change per unit distance in these gradients is typically 22 mTesla/m.

Combining a frequency gradient with a pulse of the appropriate frequency and bandwidth can excite a small slice of the sample, allowing a slice by slice investigation of the sample. If the signal is acquired immediately after slice selection, its spectrum would be a one-dimensional projection of spin density for the spins in the selected slice. To produce a two-dimensional image of spin densities in the sample, encoding along a second axis is required. While along the first axis locations are encoded by frequencies, locations along the second axis are encoded by phase.

Location-dependent phase is achieved by temporarily switching on a linear gradient along the second axis. An effect of any gradient is an enhanced dephasing of transverse magnetisation ( $M_{xy}$ ). During gradient application, local magnetisation vectors will rotate with different frequencies depending on their positions within the gradient. These spins will possess different histories, reflected in phase differences among their magnetisation vectors dependent on their positions along this second axis. The duration of the applied phase encoding gradient dictates the degree to which local transverse magnetisations are dephased. A series of increasing gradient pulse lengths will enable a reconstruction of the frequencies giving rise to the dephasing of transverse magnetisation. Hence, despite the fact that phase is being manipulated in the second axis, the amplitudes of spin frequencies are again determined and expressed as a spin density projection along the phase encode axis.

In summary, a typical imaging procedure starts with slice-selective excitation by the temporary application of a slice-selection gradient. Frequency encoding is determined by applying the frequency encoding gradient in the  $x$  axis (conventionally) during acquisition. This is followed by phase encoding along a second orthogonal axis ( $y$  axis). During image acquisition, locations are encoded by both frequency and phase of the detected signal.

### 2.26 Voxels

Step-wise increases in both gradients divide the sample into small cubes, or voxels (volume-elements). Spins in one voxel experience the same frequency and phase encoding. The signal of a given voxel is the sum of all spin contributions

hence spins within a voxel cannot be distinguished from each other. The resolution of the image depends on the size of the voxels, which is determined by the step size of the gradients. Increasing the size of the voxel increases its signal and therefore its signal to noise. However, larger voxels are more likely to encompass groups of spins with very different behaviour, which could evoke a misleading signal (referred to as the partial volume effect).

### *2.27 Image contrast*

Image contrast is based on the difference in signal intensity between areas of different structure or composition in an image. The MR signal intensity from a given voxel arises from a complex interaction of many different factors including T1 and T2 relaxation times, proton density, RF pulse characteristics and magnetic susceptibility (magnetic susceptibility refers to the fact that the net field experienced by a given nucleus depends on other magnetic spins or electron clouds in their environments). The relative contribution of some of these factors to the transverse magnetisation may be manipulated by controlling the timing of the RF pulses (known as pulse sequence parameters). The timing parameters are the repetition time (TR; the time required to acquire each image volume, i.e. the time between two consecutive 90° RF pulses) and echo time (see earlier). For example, a short TR and TE will emphasise the T1 characteristics of the tissue and produce a “T1 weighted” image. A long TR and TE produce a “T2 weighted image”.

### *2.28 Ultrafast MRI sequences: Echo-Planar Imaging*

The most commonly used MRI acquisition parameters are the spin-echo (SE) sequences. However, SE sequences can take up to minutes to acquire each slice.

Improving the speed of MRI acquisition is important for imaging dynamic processes. Although gradient-recalled echo (GRE) sequences brought imaging time down to seconds (Hasse *et al.*, 1986), the introduction of echo-planar imaging (EPI; Mansfield, 1977) sequences meant that it was theoretically possible to obtain a whole brain image in a fraction of a second.

The major difference between EPI and other MR imaging sequences is the way in which the data is sampled. Once acquired, MRI imaging data is Fourier transformed. The Fourier transform converts MR data from the time domain to the frequency domain. The two orthogonal gradients applied during phase encoding and frequency encoding means that MRI data must be considered as lying in 2-dimensional frequency space (or  $k$  space). Typical MR sequences sample one line of 2D  $k$  space after each RF pulse, whereas EPI measures all lines of  $k$  space after a single excitation. EPI therefore greatly reduces imaging time and makes it an ideal sequence for dynamic MRI techniques such as fMRI.

All experiments in this thesis were conducted at the Wellcome Department of Cognitive Neurology, Institute of Neurology, London, using a Siemens VISION system (Siemens, Erlangen), operating at 2T. This system was used to acquire both T1-weighted anatomical images and gradient-echo echo-planar T2\*-weighted MRI image volumes with blood oxygenation level dependent (BOLD) contrast.

## 2.3 fMRI and the magnetic properties of blood

### 2.3.1 BOLD contrast in fMRI

The cellular component of blood contains red blood cells (erythrocytes) which contain haemoglobin, the protein responsible for oxygen transport. Oxygen binds to iron, a constituent of the haem component of haemoglobin. When haemoglobin has no oxygen bound, each haem group has a net magnetic moment because of iron's 4 unpaired electrons (Pauling and Coryell, 1936). As soon as oxygen is bound, this net moment disappears due to a redistribution of the available electrons between iron and oxygen. The magnetic state of blood will therefore reflect its level of oxygenation.

The  $T_2^*$  of water protons is influenced by interactions between the protons themselves and also by local  $B_0$  inhomogeneities caused by different magnetic properties of various molecules. Paramagnetic molecules, such as deoxyhaemoglobin, have a local magnetic field gradient. This local gradient will contribute to the decay of transverse magnetisation and consequently shorten the  $T_2^*$  decay time. Hence changes in the levels of deoxyhaemoglobin (more precisely, changes in the ratio of deoxyhaemoglobin to oxyhaemoglobin) should result in changes in  $T_2^*$ . This effect was demonstrated empirically *in vivo* in animal work carried out by Ogawa and colleagues (Ogawa and Lee, 1990; Ogawa *et al.*, 1990) and Turner and colleagues (1991). Both groups showed that experimental manipulation of the oxy- to deoxyhaemoglobin ratio (usually by hypoxia) produced detectable contrast changes in blood vessels and, critically, within the tissue water surrounding vessels. Ogawa and colleagues (1992) and Kwong and colleagues

(1992) went on to demonstrate that the difference in T2\* signal produced by deoxyhaemoglobin concentrations *in vivo* in humans was sufficient to act as a contrast source. This signal source was termed the blood oxygenation level dependent (BOLD) contrast.

### 2.32 Neurophysiology and BOLD

The relationship between increases in neuronal electrical activity and change in blood oxygenation is still not fully understood (see Villringer and Dirnagl, 1995 for review). There is, however, agreement on the following causal chain of events. Task-related neuronal activity increases in specific areas of brain grey matter. The rates of oxygen and glucose usage in these areas are increased (Hyder *et al.*, 1997) causing a decrease in blood oxygenation in the capillary bed supplying the neuronally active tissue (Vanzetta and Grinvald, 1999) approximately 100ms after sensory stimulation. This evokes a release of vasodilatory compounds, producing increased blood flow to, and dilation of, these capillaries (Duelli and Kuschinsky, 1993). The oxygen supply to electrically active tissue begins to exceed demand and blood oxygenation increases in the capillaries and venules that drain them (Villringer and Dirnagl, 1995). If enhanced neuronal activity continues, vascular and metabolic changes reach equilibrium in 1-3 minutes. If, however, neuronal activity returns to baseline, blood flow also returns to baseline, but blood volume in draining venules remains elevated for 30-60 s after blood flow has re-equilibrated (Mandeville *et al.*, 1999).

These observations suggest a triphasic model of the BOLD response. The initial, transient decrease in oxygenation produces a small, transient decrease in the

BOLD response (the 'initial dip'). Next, local blood volume increases and thirdly, local blood flow increases 500 ms – 1 s after sensory stimulation. This third phase of the neurovascular response causes a much larger decrease in deoxyhaemoglobin concentrations than the initial increase (around x4). The BOLD contrast increase evoked by this deoxyhaemoglobin decrease is the signal that is typically measured in fMRI experiments.

The dynamics of the neurovascular response cause the BOLD signal to be delayed in time. Whereas neuronal dynamics occur in the millisecond time frame, the BOLD response takes a number of seconds to evolve. This means that although several fMRI images can theoretically be acquired in a second, the temporal smoothing of the underlying neuronal signal, effected by the BOLD response, ultimately dictates fMRI's effective temporal resolution. The time course of the neurovascular response must be accounted for in the statistical analysis of fMRI time series (see Chapter 2 part II).

As blood occupies only a small fraction of grey matter, BOLD signal changes are of the order of a few percent at best. These small signal changes require the implementation of sophisticated image processing and analysis techniques to ensure that observations reflect true BOLD signal and not noise. These techniques are described in the next section.